A Brownian Dynamics Study of the Interaction of *Phormidium* Cytochrome *f* with Various Cyanobacterial Plastocyanins

Elizabeth L. Gross and Irving Rosenberg
Department of Biochemistry, The Ohio State University, Columbus, Ohio

ABSTRACT Brownian dynamics simulations were used to study the role of electrostatic forces in the interactions of cytochrome *f* from the cyanobacterium *Phormidium laminosum* with various cyanobacterial plastocyanins. Both the net charge on the plastocyanin molecule and the charge configuration around H92 (H87 in higher plants) are important in determining the interactions. Those plastocyanins (PCs) with a net charge more negative than −2.0, including those from *Synechococcus* sp. PCC7942, *Synechocystis* sp. 6803, and *P. laminosum* showed very little complex formation. On the other hand, complex formation for those with a net charge more positive than −2.0 (including *Nostoc* sp. PCC7119 and *Prochlorothrix hollandica*) as well as *Nostoc* plastocyanin mutants showed a linear dependence of complex formation upon the net charge on the plastocyanin molecule. Mutation of charged residues on the surface of the PC molecules also affected complex formation. Simulations involving plastocyanin mutants K35A, R93A, and K11A (when present) showed inhibition of complex formation. In contrast, D10A and E17A mutants showed an increase in complex formation. All of these residues surround the H92 (H87 in higher plant plastocyanins) ligand to the copper. An examination of the closest electrostatic contacts shows that these residues interact with D63, E123, R157, D188, and the heme on *Phormidium* cytochrome *f*. In the complexes formed, the long axis of the PC molecule lies perpendicular to the long axis of cytochrome *f*. There is considerable heterogeneity in the orientation of plastocyanin in the complexes formed.

INTRODUCTION

Cytochrome *f* (cyt *f*) is a member of the cytochrome b_6f complex (1–4). It accepts electrons from the Rieske FeS protein and donates them to plastocyanin (PC). PC is a blue copper protein which is a mobile electron carrier located in the lumen of the thylakoid, where it accepts electrons from cyt *f* and donates them to P700 in Photosystem I (5–11).

Electrostatic interactions have been shown to be very important for complex formation between cyt *f* and PC from higher plants using chemical modification (12–14), cross-linking (15–17), and mutagenesis techniques (18–21). In contrast, mutagenesis studies of cyt *f* from the green alga *Chlamydomonas* demonstrated that electrostatic interactions were not important in *Chlamydomonas* in vivo (22), although they were observed in vitro (20).

Higher plant cyt *f*s have a positively-charged electrostatic field (23) due to a series of highly conserved positively charged residues (K58, K65, K66, K187, and R209 in turnip cyt *f*) (24–26), which interact with the negatively-charged electrostatic field on higher plant PCs (27) caused by two clusters of anionic residues (7,8) on PC. In cyanobacterial cyt *f*s, such as that of *Phormidium laminosum*, the cationic residues are replaced by anionic residues (1,28) and the anionic patches on PC are replaced by cationic or neutral residues (Fig. 1) (29–35). The net charge on cyanobacterial PCs varies over a wide range. *Prochlorothrix hollandica* and *Nostoc* sp. PCC7119 (formerly *Anabaena variabilis*) PCs have a net charge of 1.1 and 1.0 at pH 7.0, respectively, as calculated using the program MacroDox (36). Positively-charged residues on these PC molecules, including R93 (consensus sequence; see Appendix), K11, and K35 surround the H92 ligand to the copper atom resulting in a positively-charged electrostatic field over the top of the molecule (Fig. 1 *A*). In contrast, *Phormidium* PC has a net charge of −2.3 at pH 7.0 and shows a much reduced positive patch surrounding H92 (Fig. 1 *A*). The PCs from *Synechocystis* sp. PCC6803 and *Synechococcus* sp. PCC7922, with a net charge of −1.8 and −4.5, respectively, have a negative electrostatic field except in the vicinity of H92 and R93 (Fig. 1 *B*).

The role of the electrostatic interactions in complex formation between *Phormidium* cyt *f* and both *Phormidium* PC (37) and *Prochlorothrix* PC (38) has been studied using NMR spectroscopy. Complex formation between *Prochlorothrix* PC and *Phormidium* cyt *f* was dependent on the salt concentration indicating the presence of electrostatic interactions whereas the interaction of *Phormidium* PC, also with *Phormidium* cyt *f*, showed no salt dependence—suggesting that, in this case, electrostatic interactions do not play an important role in complex formation. However, Schlarb-Ridley et al. (34) observed that mutation of charged residues on *Phormidium* PC did affect the rate of electron transfer from *Phormidium* cyt *f* to *Phormidium* PC, suggesting that electrostatic interactions do play a role.

In this article, we will use Brownian dynamics (BD) simulations (35,36,39) to examine the relationship between the net charge on five PC molecules from five different species of cyanobacteria (*Prochlorothrix hollandica*, *Nostoc* sp. PCC7119, *Phormidium laminosum*, *Synechocystis* sp. PCC6803, and *Synechococcus* sp. PCC7942) and their ability to form complexes with *Phormidium laminosum* cyt *f*. We show that electrostatic interactions between cyt *f* and PC depend on two factors: 1), the net charge on the PC molecule;

Submitted April 22, 2005, and accepted for publication September 13, 2005.
Address reprint requests to Elizabeth L. Gross, E-mail: gross.3@osu.edu.

0006-3495/06/01/366/15 $2.00
doi: 10.1529/biophysj.105.065185

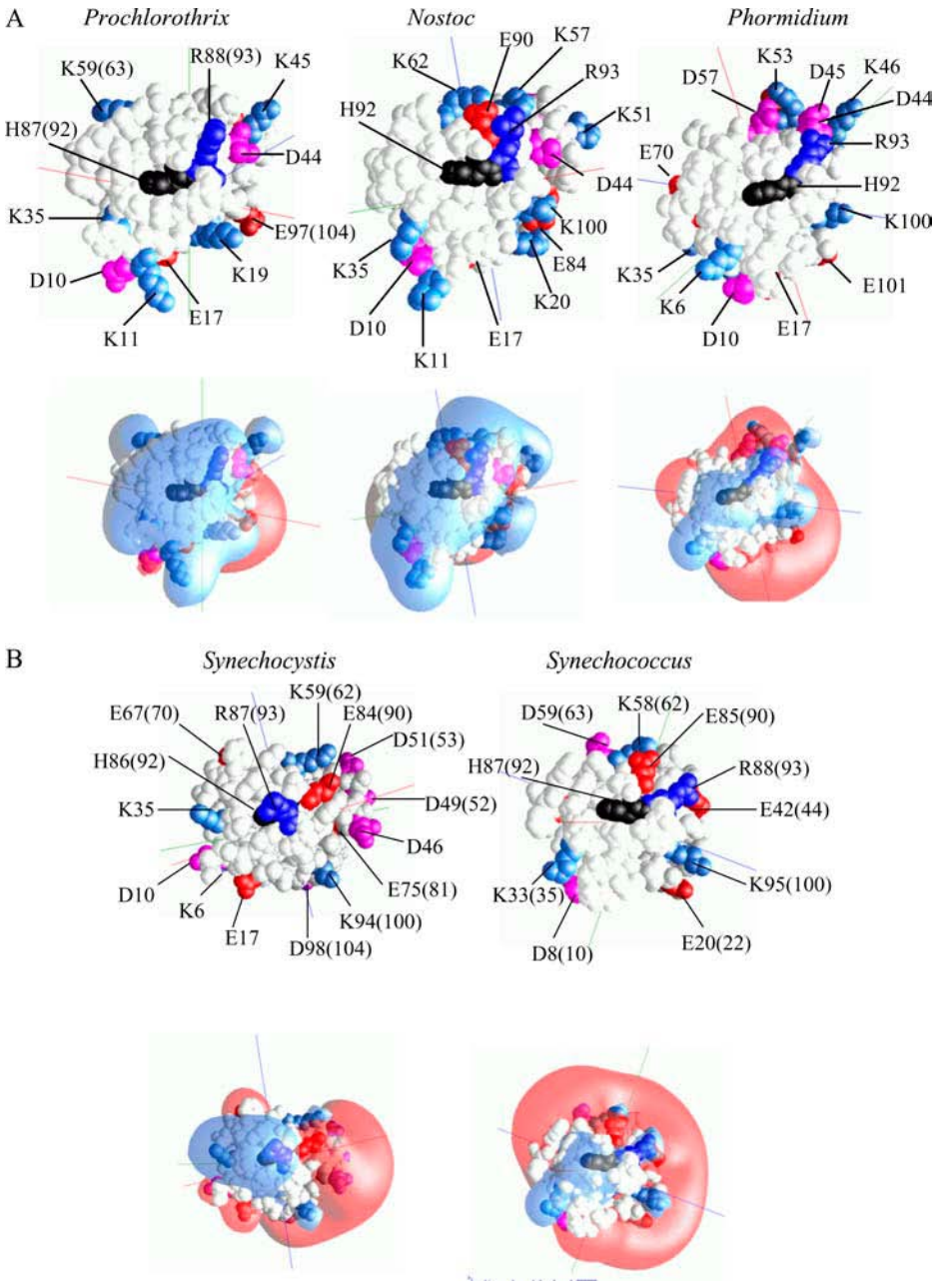

FIGURE 1 Cyanobacterial plastocyanins. (*A*) (*Top row*) View of cyanobacterial PCs looking down on the H92 (consensus sequence) view of three cyanobacterial plastocyanins (*Prochlorothrix*, *Nostoc*, and *Phormidium*) showing charged residues. (H92, *black*; arginine, *dark blue*; lysine, *light blue*; glutamate, *red*; and aspartate, *magenta*.) (*Bottom row*) Electrostatic fields at 1 kT/e^- (*blue*) and −1 kT/e^- (*red*) for the five plastocyanins. (*B*) *Synechocystis* and *Synechococcus* PC. Other conditions are the same as for Fig. 1 *A*.

and 2), the distribution of charged residues surrounding H92 on the surface of the PC molecule, which will, in turn, allow us to show that cyanobacterial PCs possess a common binding site for *Phormidium* cyt *f*.

BD simulations have been used to study the interaction of turnip cyt *f* with poplar (40) and spinach PC (41,42); *Chlamydomonas* cyt *f* interacting with *Chlamydomonas* PC (43,44); and *Phormidium* cyt *f* interacting with *Phormidium* PC (35). Brownian dynamics simulations of the interaction between *Phormidium* PC and *Phormidium* cyt *f* (35) showed that fewer complexes were formed than for the green alga *Chlamydomonas reinhardtii* PC interacting with *Chlamydomonas* cyt *f*, unless the Zn^{2+} ion found in the crystal structure of *Phormidium* PC (31) was included in the simulations. However, even in the absence of the Zn^{2+} ion, mutation of charged residues on *Phormidium* PC and cyt *f* affected the rate of complex formation in BD simulations.

METHODS

Molecular structures

The protein structures were obtained from the Protein Data Bank (PDB) (http://www.rcsb.org/pdb/ (45)). *Phormidium laminosum* cyt *f* (structure 1CI3) was taken from Carrell et al. (28). The *Phormidium laminosum* PC used was structure A (1BAW) from Bond et al. (31); the *Prochlorothrix hollandica* PC

used was the minimized average NMR structure (1B3I) of Babu et al. (30); the *Nostoc* sp. PCC7119 (formerly *Anabaena variabilis*) PC used was structure 3 of 1NIN from Badsburg et al. (29); the *Synechocystis* PCC6803 PC structure was the minimized average structure (1J5D) taken from Bertini et al. (32), and the *Synechococcus* sp. PCC7922 PC structure (1BXU) was taken from Inoue et al. (33). The structure of *C. reinhardtii* cyt *f* used (1CFM) was structure B from Chi et al. (46) and that of *Chlamydomonas* PC (2PLT) was that of Redinbo et al. (47).

Structures for mutant molecules were generated using the MacroDox program (36,48,49). All mutant residues were kept in the same orientation as their wild-type counterparts (i.e., no energy minimization was performed on the mutants). Mutants were divided into different classes depending on their relative effects (See Tables 1 and 2).

Molecular representations

All molecular representations were made using the program GRASP (50). Electrostatic fields for the molecular representation only were also calculated using GRASP. The internal and external dielectric constants of the proteins were 4 and 78, respectively. The ionic strength was 10 mM and the pH was 7.0.

Brownian dynamics (BD) simulations

BD simulations were carried out using the program MacroDox v. 3.2.1 (http://gemini.tntech.edu/~s;/index.html), as described (35,40,43,51). In MacroDox simulations, target molecule (Molecule I, in our case, cyt *f*) is placed with its center of mass at the center of a sphere 87 Å in diameter (87 Å was chosen so that the initial electrostatic fields would be very small). Molecule II (in our case, PC) is placed randomly on the surface of the sphere. Molecule II is allowed to move in response to both electrostatic and random Brownian forces. After Molecule II has moved an incremental distance, the forces are recalculated. The steps form a trajectory which ends when Molecule II leaves a sphere of 200 Å in diameter, with its center at the center-of-mass of the target molecule.

MacroDox determines the closest approach of the two molecules for each trajectory based on a preselected reaction criterion. Closest metal-to-metal distance was chosen as the reaction criterion to select for electron-transfer-active complexes (52,53). The point of closest approach (smallest Cu-Fe distance) was recorded for each trajectory, permitting the calculation of the number of complexes formed as a function of minimal Cu-Fe distance (Fig. 2). Second-order rate constants for complex formation were calculated from the fraction of complexes observed at distances less than or equal to a preselected reaction criterion using equations derived by Northrup et al. (36,48) from the equations of Smoluchowski. If the reaction is diffusion-limited, as was suggested by Hart et al. (54), the rate of complex formation (k_2) should be equal to the rate constant for electron transfer (k_{et}) However, this may not be true in this case (55) (see Discussion). The number of complexes with a Cu-Fe distances of $\leq$20 Å was used to calculate the rate constants; 20 Å was sufficient to include essentially all of the electrostatic complexes formed while excluding those formed solely by random Brownian motion (Fig. 2). MacroDox provides the following information for each trajectory: The structure of the complex at minimum Cu-Fe distance, the 15 closest pairs of charged residues, and the electrostatic interaction energy.

Charge assignments and electrostatic calculations used in MacroDox simulations

Formal charges were assigned to ionizable groups such as amino, carboxyl, guanido, and imidazole groups. Partial charges were not assigned to polarizable atoms such as oxygen and nitrogen since the inclusion of partial charges had a negligible effect on the number of complexes formed in the interaction of *Chlamydomonas* cyt *f* with *Chlamydomonas* PC (43).

When using formal charges, noninteger values of the charge on PC and cyt *f* result from the ionization of histidine residues at pH 7. H25 on cyt *f* and H39 and H92 (see Appendix) on PC have a zero net charge because they are ligands to the metal centers. The sulfur atom of the Cys-89 ligand to the Cu on PC was given a net charge of -1 (27), and the Cu atom was given a charge of $+2$. For cyt *f*, the charges on the heme were as follows: Fe ($+2$), two ring nitrogen atoms (-1 each), and two propionic acid side chains (-1 each). The pK values were calculated using a modified Tanford-Kirkwood pK algorithm (56).

Electrostatic calculations were carried out using the Warwicker/Watson finite difference method (57) for solving the linearized Poisson-Boltzmann equation. This algorithm is slightly different from that used in GRASP. The

TABLE 1 The effect of mutation of charged residues on *Prochlorothrix* PC on its interaction with *Phormidium* cyt *f*

Class*	Mutant	Number of complexes formed per 1000 trajectories	Percentage of WT	$10^{-8} \times k_a$ (M^{-1} s^{-1})†
	WT	341.8 ± 5.1	100 ± 2.0	85.7 ± 2.9
Class I	D10A	469.0 ± 7.9	137.2 ± 3.2	108.9 ± 2.8
	E17A	447.6 ± 6.5	131.2 ± 2.8	105.2 ± 3.3
	D44A	447.4 ± 7.2	130.9 ± 2.9	105.1 ± 3.0
Class II	E30A	414.2 ± 5.5	121.2 ± 2.5	99.4 ± 3.2
	E50[54]A	412.6 ± 6.1	120.7 ± 2.6	99.1 ± 3.2
	E97[104]A	402.4 ± 6.4	117.7 ± 2.6	97.2 ± 3.0
	D27A	398.8 ± 3.7	116.7 ± 2.1	96.5 ± 3.3
Class III	K6A	246.4 ± 7.3	72.1 ± 2.4	65.5 ± 2.8
	K59[63]A	230.2 ± 5.5	67.3 ± 1.9	62.0 ± 3.2
	K45A	228.4 ± 4.4	66.8 ± 1.7	61.6 ± 2.9
Class IV	K19A	206.4 ± 8.3	60.4 ± 2.6	56.4 ± 3.3
	K11A	196.4 ± 4.2	57.5 ± 1.5	53.2 ± 3.1
	K35A	177.8 ± 2.0	52.0 ± 1.0	49.6 ± 2.8
Class V	R86[93]A	123.6 ± 4.3	36.2 ± 1.5	35.8 ± 2.2
	WT-field off	1.8 ± 0.7	0.5 ± 0.2	1.1 ± 0.7

*The mutants were divided into classes based on their effects on complex formation: *Class I*, significant stimulation (i.e., the number of complexes formed was $\geq$130% of that of the WT); *Class II*, moderate stimulation (100–130% of WT complex formation); *Class III*, moderate inhibition of complex formation (60–100% of WT); *Class IV*, strong inhibition (45–65% of WT complex formation); and *Class V*, very strong inhibition ($<$45% WT complex formation). The ionic strength was 10 mM. Five sets of 1000 trajectories were carried out.

†The rates of electron transfer were calculated as described in Methods, based on the number of complexes formed with Cu-Fe distances $\leq$20 Å.

TABLE 2 The effect of mutation of charged residues on *Nostoc* PC (formerly *Anabaena*) on its interaction with *Phormidium* cyt *f*

Class*	Mutant	Number of complexes formed per 1000 trajectories	Percentage of WT	$10^{-8} \times k_a$ (M^{-1} s^{-1})†
	WT	325.6 ± 5.5	100 ± 1.7	80.5 ± 2.9
Class I	D10A	459.4 ± 3.4	141.1 ± 2.6	105.2 ± 2.5
	E17A	450.2 ± 3.4	138.3 ± 2.5	103.8 ± 2.3
	E90A	445.6 ± 4.9	136.9 ± 2.7	101.7 ± 2.3
	D44A	439.2 ± 5.6	134.9 ± 2.8	100.6 ± 3.0
Class II	E84A	419.2 ± 1.4	128.7 ± 2.2	97.2 ± 2.8
	E30A	406.8 ± 6.9	124.9 ± 3.0	96.2 ± 3.0
	D54A	400.8 ± 5.6	123.1 ± 2.7	93.9 ± 3.0
	D27A	389.6 ± 5.9	119.7 ± 2.7	92.5 ± 2.5
	D79A	385.6 ± 4.7	118.4 ± 2.5	91.2 ± 2.7
	E1A	380.5 ± 2.6	116.9 ± 2.1	91.3 ± 3.0
Class III	K24A	270.2 ± 4.9	83.0 ± 2.1	69.2 ± 3.1
	K20A	244.6 ± 5.7	75.1 ± 2.2	63.7 ± 3.3
	K51A	231.4 ± 6.6	71.1 ± 2.3	60.5 ± 2.8
	K100A	221.4 ± 7.2	68.0 ± 2.5	58.2 ± 2.9
	K57A	210.0 ± 5.4	64.5 ± 2.0	55.6 ± 3.2
	K6A	200.8 ± 2.5	61.7 ± 1.3	54.3 ± 3.1
Class IV	K35A	186.8 ± 5.5	57.4 ± 1.9	50.8 ±3.3
	K11A	180.8 ± 8.2	55.5 ± 2.7	47.4 ± 3.5
	K62A	176.8 ± 6.7	54.3 ± 2.2	47.9 ± 3.0
Class V	R93A	135.2 ± 4.0	41.5 ± 1.4	37.8 ± 2.7
	WT-field off	7.8 ± 1.0	2.4 ± 0.3	4.9 ± 0.2

*The mutants were divided into classes based on their effects on complex formation: *Class I*, significant stimulation (i.e., the number of complexes formed was ≥130% of that of the WT); *Class II*, moderate stimulation (100–130% of WT complex formation); *Class III*, moderate inhibition of complex formation (60–100% of WT); *Class IV*, strong inhibition (45–65% of WT complex formation); and *Class V*, very strong inhibition (<45% WT complex formation). The ionic strength was 10 mM. Five sets of 1000 trajectories were carried out.

†The rates of electron transfer were calculated as described in Methods, based on the number of complexes formed with Cu-Fe distances ≤20 Å.

center-of-mass of each protein was placed at the center of a 61 × 61 × 61 grid. The electrostatic field was first iterated over a 3.6 Å grid followed by iteration over a smaller 1.2 Å grid for better accuracy. The choice of grid size has a small (<20%) effect on the rates, but no effect on the structure of the complexes formed (43). Most importantly, the relative rates of electron transfer were not affected.

Forces, torques, and electrostatic interaction energies

Forces were calculated as described by Northrup et al. (36). Molecule I (cyt *f*, the target molecule) was given a low internal dielectric constant of 4.0. However, because of computational complexities, Molecule II (PC) was treated as a set of point charges embedded in a medium of the same dielectric (48,58,59) (S. Northrup, personal communication, 2002). Also, mutual desolvation effects (59,60) were neglected. These effects may cause an overestimation of the reaction rates by as much as 25%. However, desolvation effects are not significant in these simulations (35). By neglecting these, neither the relative effects of the mutations nor the structures of the complexes formed should be affected (48) (S. Northrup, personal communication, 2002). Also, hydrodynamic effects can be neglected due to the compact nature of the molecules (39). Torques were calculated using dipoles for the moving protein as described by Northrup et al. (61).

Calculation of hydrophobic and electrostatic free energies

Hydrophobic interaction free energies were determined as described by Gross and Pearson (43). The residues at the complex interfaces were determined by selecting those residues on *Phormidium* cyt *f* within 8 Å of any residues on PC (10 Å for *Phormidium* PC), using an in-house program. Those residues on PC within 8 Å (10 Å for *Phormidium* PC) of any residue on cyt *f* were chosen using the same method. Ten representative complexes, with Cu-Fe distances less than or equal to those at maximum complex formation, were chosen for study (17 Å for *Nostoc* and *Prochlorothrix* Y12G PC, 18 Å for WT *Prochlorothrix* PC and 21 Å for *Phormidium* PC). A residue was considered to be part of the interface if it was observed in at least eight of the 10 complexes chosen (seven out of 10 complexes for *Phormidium* PC). The calculated interaction area is an underestimate, particularly in the case of *Phormidium* PC, because the two molecules are not as close as they will be in the final electron transfer active dock. The surface areas of the hydrophobic atoms of these residues on both PC and cyt *f* were calculated using the Richards (62,63) algorithm, which is part of the MacroDox software package. The total hydrophobic surface area was considered to be twice the smaller of the PC or cyt *f* hydrophobic surface area.

Reported values for hydrophobic interaction energies vary between −25 and −47 cal/Å^2 (64–66). Because of the wide variation, both −25 and −47 cal/Å^2 were used for our calculations.

Electrostatic interactions were taken from the .rec files of the MacroDox output. In each case, all complexes formed with Cu-Fe values less than the values of maximal complex formation (see above) were included. Five sets of 1000 trajectories for *Prochlorothrix* and *Nostoc* and 5000 trajectories for *Phormidium* PC were averaged and included between 150 and 400 complexes per set.

RESULTS

Comparison of complex formation for five cyanobacterial PCs interacting with cyt *f* from *Phormidium laminosum*

In these studies (Fig. 2), the number of complexes formed was determined as a function of minimum Cu-Fe distance for cyt *f* interacting with PCs from several cyanobacteria at 10 mM ionic strength and pH 7.0. In all of these plots, the point at 17 Å shows the number of complexes in which the minimum distance between the Cu on PC and the Fe on cyt *f* was between 16 and 17 Å.

Fig. 2 *A* compares the results for *Nostoc*, *Prochlorothrix*, and *Phormidium* PC interacting with *Phormidium* cyt *f*, with those previously obtained for *Chlamydomonas* PC interacting with *Chlamydomonas* cyt *f* (43). In the case of *Nostoc* PC, maximum complex formation occurred at a Cu-Fe distance of 17 Å compared to 15 Å for the *Chlamydomonas* system. However, for *Prochlorothrix* PC, the peak is shifted to 18 Å as a result of the presence of a tyrosine at position #12 in *Prochlorothrix* PC instead of the glycine found in PCs from all other species (8). When Y12 is replaced by a glycine (Fig. 2 *B*), the peak is shifted back to 17 Å. The double mutant (Y12G + P14L) described by Crowley et al. (38) showed nearly identical results to the single Y12G mutant. Both *Nostoc* and *Prochlorothrix* PC showed a greater number of complexes formed when interacting with *Phormidium* cyt *f*

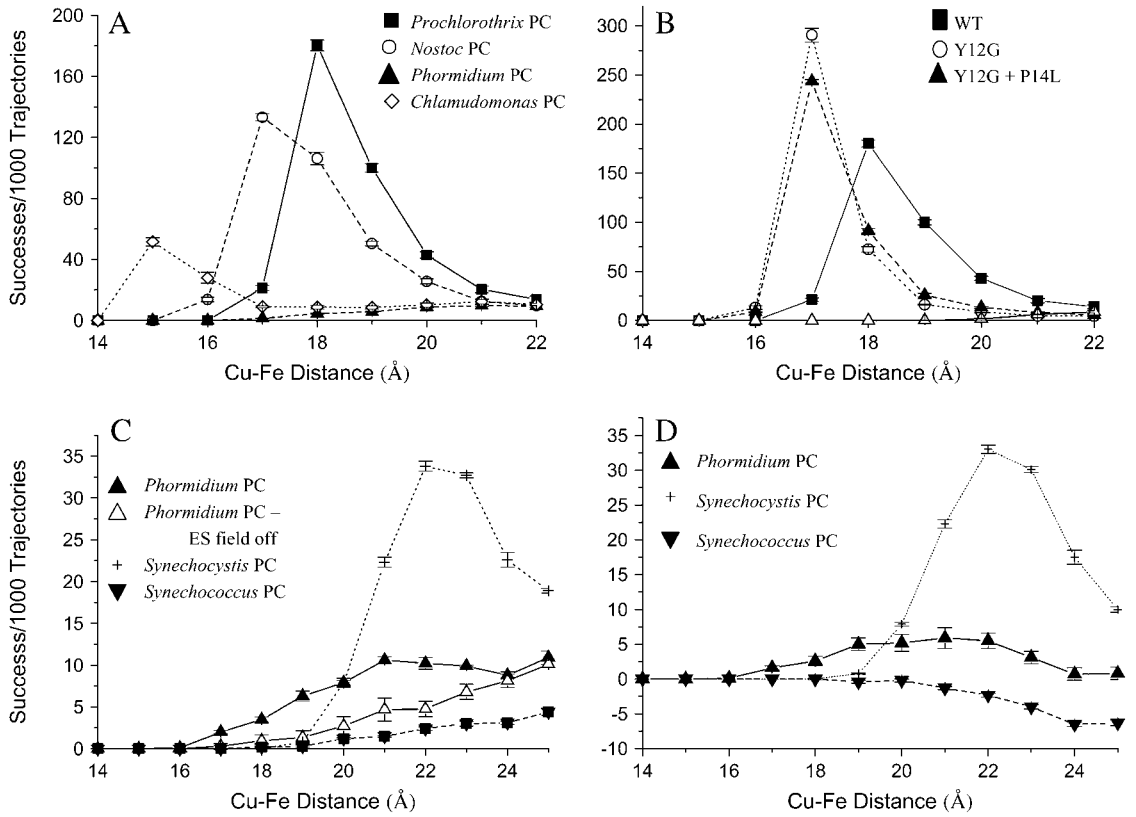

FIGURE 2 The number of complexes formed in BD simulations as a function of Cu-Fe distance for *Phormidium* cyt *f* interacting with PCs from different species of cyanobacteria. (*A*) Comparison of *Prochlorothrix*, *Nostoc*, and *Phormidium* PC interacting with *Phormidium* cyt *f* with *Chlamydomonas* PC interacting with *Chlamydomonas* cyt *f* (Structure *B* from Chi et al. (46)). Five sets of 5000 trajectories were carried out for *Phormidium* PC. (*B*) The effect of Y12G and Y12G+P14L mutations on the number of complexes formed for *Prochlorothrix* PC interacting with *Phormidium* cyt *f*. (*C*) A comparison of the number of complexes formed for *Phormidium* PC, *Phormidium* PC with the electrostatic field turned off; *Synechocystis* PC, and *Synechococcus* PC interacting with *Phormidium* cyt *f*. Five sets of 10,000 trajectories were carried out for *Synechocystis* and *Synechococcus* PC and for all PCs studied in the absence of the electrostatic field. (*D*) A comparison of the number of complexes formed for *Phormidium* PC, *Synechocystis* PC, and *Synechococcus* PC interacting with *Phormidium* cyt *f* after subtractions of the number of complexes formed in the absence of the electrostatic field for that species. Conditions were the same as for Fig. 2 *C*.

than did *Chlamydomonas* PC interacting with *Chlamydomonas* cyt *f* (Fig. 2 *A*).

When *Phormidium* PC interacted with *Phormidium* cyt *f*, peak complex formation was shifted to 20 Å (Fig. 2 *D*). Also, the number of complexes formed was only 20.4 ± 0.5 complexes/1000 trajectories compared to 341.2 ± 4.7 for *Prochlorothrix* PC under the same conditions. However, in the absence of the electrostatic field, the number of complexes formed were 2.0 ± 0.2 (35) and 1.8 ± 0.8 (Table 1) for *Phormidium* and *Prochlorothrix* PC, respectively, indicating that the differences in complex formation reflect the differences in charge on the two PC proteins. Maximum complex formation was observed at a Cu-Fe distance of 22 Å (with a value of 33.7 ± 0.6 complexes/1000 trajectories) for *Synechocystis* PC (Fig. 2 *D*).

Interestingly, in the case of *Synechococcus* PC, fewer complexes were formed in the presence of the electrostatic field than in its absence (Fig. 2, *C* and *D*), indicating charge repulsion between *Synechococcus* PC and *Phormidium* cyt *f*. This is not surprising, since the net charge on *Synechococcus* PC is −4.5 compared to a net charge −14.0 *Phormidium* cyt *f*. This raises the questions as to whether *Synechococcus* PC would show greater complex formation when interacting with *Synechococcus* cyt *f* than with *Phormidium* cyt *f*. For this reason, *Synechococcus* cyt *f* was built by homology-modeling with SWISS MODEL ((67) http://swiss-model.expasy.org), using turnip and *Phormidium* cyt *f* as templates. When *Synechococcus* PC interacted with *Synechococcus* cyt *f*, 17.1 ± 0.1 complexes with Cu-Fe distances ≤20 Å were formed per 1000 trajectories compared to 18.0 ± 0.1 for *Phormidium* cyt *f* under the same conditions. The rates of interaction were 4.9 ± 1.3 and 5.3 ± 1.0 × 10^7 M^{-1} s^{-1}, respectively. These results are not surprising since the net charge on the *Synechococcus* cyt *f* molecule is −18.7 as calculated by MacroDox compared to −14.0 for *Phormidium* cyt *f*. Therefore, the poor performance of *Synechococcus* PC can not be attributed to using the ''wrong'' cyt *f*.

The effect of the net charge on the PC molecule on the number of complexes formed with *Phormidium* cyt *f*

One reason for the difference in the number of complexes formed for PCs from different species of cyanobacteria may be the difference in net charge on the various PC molecules. To test this hypothesis, two types of simulations were performed (Fig. 3). In the first experiment, indicated by the numbers *1–9* next to the data points in Fig. 3, the net charge on *Prochlorothrix* PC was varied between −2.0 and +3.0 by mutating charged residues to alanine. The results show that the number of complexes formed was a linear function of the net charge at values more positive than −1.0. The results for mutants of *Phormidium* PC also fall on the same line (68). In the second set of simulations, the five cyanobacterial PCs shown in Figs. 1 and 2 were compared. These are indicated by letters *A–D* and the number *5* on Fig. 3. It can be seen that few, if any, complexes were formed, due to electrostatic interactions alone, if the net charge on the PC molecule was more negative than −2, but that the data point for *Nostoc* PC falls on the same line as for the *Prochlorothrix* mutants. Thus, the number of complexes formed is a linear function of the net charge on the PC molecule for a net charge greater than −2. Note that, in both sets of experiments, hydrophobic interactions were not included in the simulations. If they had been, the number of complexes formed would have been greater and significant complex formation would have been observed for *Synechocystis*, *Synechococcus*, and *Phormidium* PC.

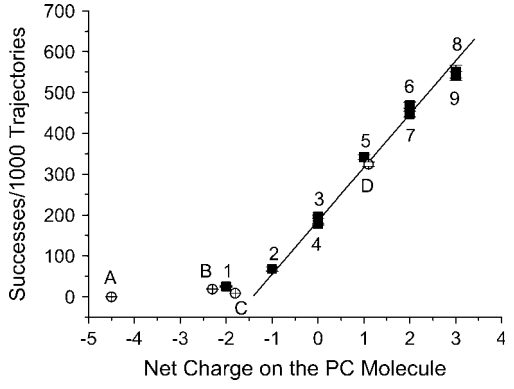

FIGURE 3 The dependence of BD complex formation on the net charge on the PC molecule. All complexes with Cu-Fe distance <20 Å were counted. The ionic strength was 10 mM and the pH was 7.0. Other conditions were as described for Fig. 2. Experiment 1: *Phormidium* cyt *f* interacting with *Prochlorothrix* PC mutants. (*1*) K35A + K11E (net charge = −2); (*2*) K35A + K11A (net charge = −1); (*3*) K35A (net charge = 0); (*4*) K11A (net charge = 0); (*5*) WT (net charge = +1.0); (*6*) D10A (net charge = +2.0); (*7*) D44A (net charge = +2.0); (*8*) D10K (net charge = +3.0); and (*9*) D44K (net charge = +3.0). Experiment 2: PC molecules from different species of cyanobacteria interacting with *Phormidium* cyt *f*. (*A*) *Synechococcus* PC (net charge = −4.5). (*B*) *Phormidium* PC (net charge = −2.3). (*C*) *Synechocystis* PC (net charge = −1.8). (*D*) *Nostoc* PC (net charge = +1.1). Net charges were calculated using MacroDox.

The effect of the location of the charged residues on the surface of the PC molecule on the number of complexes formed

A second question is whether the location of the charged residues on the surface of the PC molecule affects complex formation. If so, it should be possible to use mutations to map the binding site on PC for cyt *f* and to determine whether the binding site for cyt *f* on PC is the same for the various cyanobacterial PCs studied. Fig. 4 depicts the effect of mutation of all of the conserved residues on *Prochlorothrix*, *Nostoc*, and *Phormidium* PC plus the K11A mutation for *Prochlorothrix* and *Nostoc* PC (Residue #11 is a serine rather than a lysine on *Phormidium* PC) on the ability of PC to form complexes with *Phormidium* cyt *f*. A similar pattern was observed for all three cyanobacterial plastocyanins shown as well as for *Synechocystis* PC (not shown). In all cases, the D10A, E17A, and D44A mutations increased the number of complexes formed. In contrast, the K11A, K35A, and R93A mutants decreased complex formation. All of these residues are located on the top face of the cyanobacterial PCs surrounding H92 (which corresponds to H87 in higher plant and algal PCs; see Appendix, and Figs. 1 and 5). Note that all of the conserved charged residues are located on the top face of the PC molecule.

Tables 1 and 2 summarize the effects of mutating all of the charged residues on *Prochlorothrix* and *Nostoc* PC on their ability to form complexes *Phormidium* cyt *f*. In each case, the number of complexes formed with Cu-Fe distances ≤20 Å was determined. A 20 Å reaction criterion was chosen under the assumption that once the metal centers of the two molecules approach to within that distance, hydrophobic interactions come into play. For comparison, the PC and cyt *f* touch each other at a Cu-Fe distance of 15 Å for *Nostoc* PC and 16 Å for *Prochlorothrix* and *Phormidium* PC. Changing the reaction criterion to 18 Å changes the number of complexes included but not the relative effects of the mutations (35).

For both *Prochlorothrix* and *Nostoc* PC, the mutants were divided into five classes:

Class I contains those mutants that showed complex formation ≥130% of the WT values. These included D10A, E17A, and D44A for PCs from both species. In addition, E90A, which is not conserved, was also included in Class I for *Nostoc* PC.

Class II consists of those mutants that showed a slight stimulation of complex formation (i.e., 100–130% of WT). D27A, E30A and E54A were included for PC from both species of cyanobacteria. For *Prochlorothrix* PC, E97[104]A was also included, as were E1A, D79A, and E84A for *Nostoc* PC.

Class III includes those mutants that showed slight inhibition of complex formation (i.e., between 65 and 100% of WT). K6A was included in this class for both *Prochlorothrix* and *Nostoc* PC. K59 (63) and K45A was included in this class for *Prochlorothrix* PC whereas

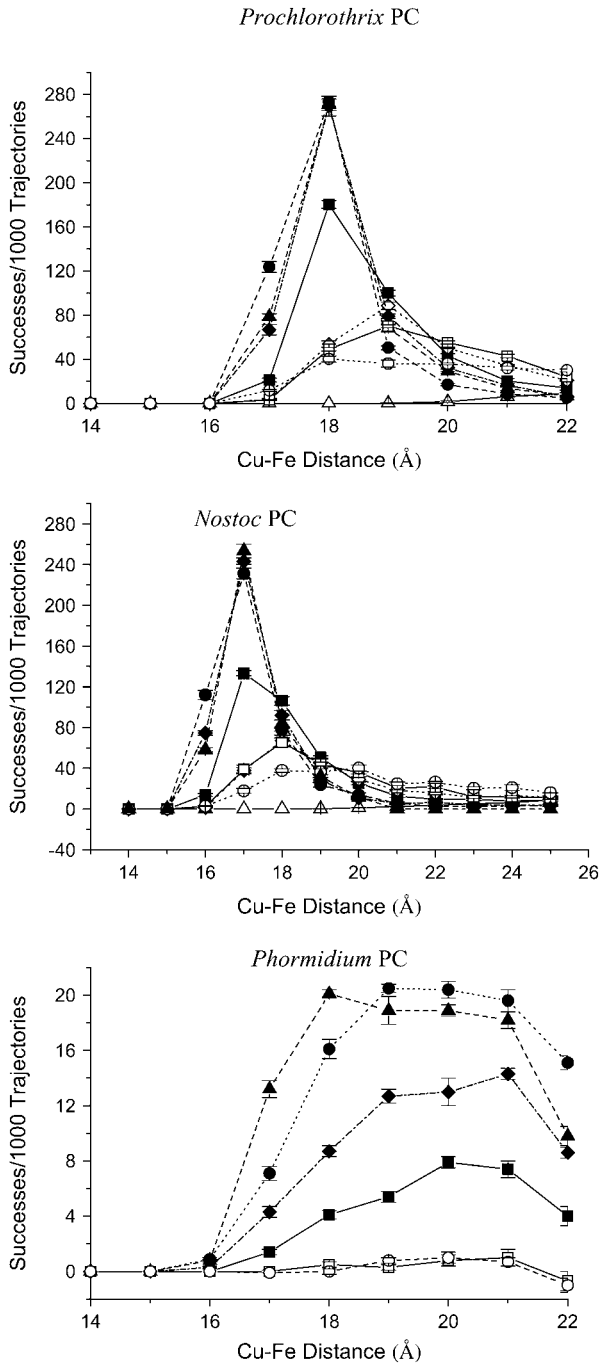

FIGURE 4 The effect of mutations of conserved charged residues on the number of complexes formed for *Prochlorothrix*, *Nostoc*, and *Phormidium* PC interacting with *Phormidium* cyt. ■ WT; △ WT = off; ▲ D44A; ● D10A; ◆ E17A; □ K35A; ○ R86A; ◇ K11A.

K20A, K24A, K51A, K57A, and K100A were included in this class for *Nostoc* PC.

Class IV consisted of those mutants with complex formation between 45 and 65% of wild-type. Class IV contains K11A and K35A for both species of cyanobacteria as well as K19A for *Prochlorothrix* PC and K62A for *Nostoc* PC.

Class V contains the one mutant with complex formation <45% for both species, namely, R93A.

D44A, D10A, and E17A also showed maximal stimulation of the interaction of *Phormidium* PC with *Phormidium* cyt *f* (35), and D10A and E17A also showed significant stimulation for *Synechocystis* PC (not shown) interacting with *Phormidium* cyt *f*. K6A, K35A, K46A, K100A, and R93A also showed severe inhibition for *Phormidium* PC interacting with *Phormidium* cyt *f* (35) as did mutants K6A, K35A, and R93A (consensus sequence) for *Synechocystis* PC (not shown). Thus, the same residues (especially D10, E17, D44, K35, R93, and possibly K6) are involved in complex formation in all four cyanobacterial PCs studied. K11 is also important for *Prochlorothrix* and *Nostoc* PC. S11K mutants of *Phormidium* and *Synechocystis* PC (not shown) stimulated complex formation to the same extent as the neighboring D10A mutants, indicating that a lysine at position 11, when present, also assists in complex formation. The locations of these important (Classes I, IV, and V) residues on the surface of *Prochlorothrix*, *Nostoc*, and *Phormidium* PC are shown in Fig. 5. Note that they all surround H93 (H87 in higher plant and algal PCs) on the top face of the PC molecule. Also, note the significant role of conserved charged residues in complex formation. Moreover, the location of these charged residues controls the location of binding site on PC for cyt *f* but the net charge on the PC molecule controls the strength of the electrostatic portion of the interaction.

Close electrostatic contacts

The output of the MacroDox program provides a list of the 15 closest electrostatic contacts for all complexes with reaction coordinate distances less than or equal to a preset value. For our studies of cyanobacterial PCs interacting with *Phormidium* cyt *f*, we chose a Cu-Fe distance less than or equal to that which gave the peak value for complex formation. This value was 20 Å for *Phormidium* PC, 17 Å for *Nostoc* PC, and 18 Å for *Prochlorothrix* PC, respectively. The results are presented in Table 3. A given residue was listed if it appeared as one of the 15 closest contacts in at least 50% of the complexes formed.

Conserved positively-charged cationic residues, K35 and R93, showed at least one contact with a residue on cyt *f* for *Prochlorothrix*, *Nostoc*, and *Phormidium* PC as well as for *Synechocystis* PC (not shown). Also, K11 showed more than one contract for *Prochlorothrix* and *Nostoc* PC that have this residue. Close contacts for nonconserved cationic residues include K19 and K59[63] for *Prochlorothrix* PC, K62 for *Nostoc* PC, and K46 for *Phormidium* PC. Close contacts for anionic residues include D10, which is observed for *Prochlorothrix* and *Phormidium* PC. E90 is also prominent in *Nostoc* PC and D44 and E70 are involved in charge repulsion in *Phormidium* PC. All of these residues (cationic

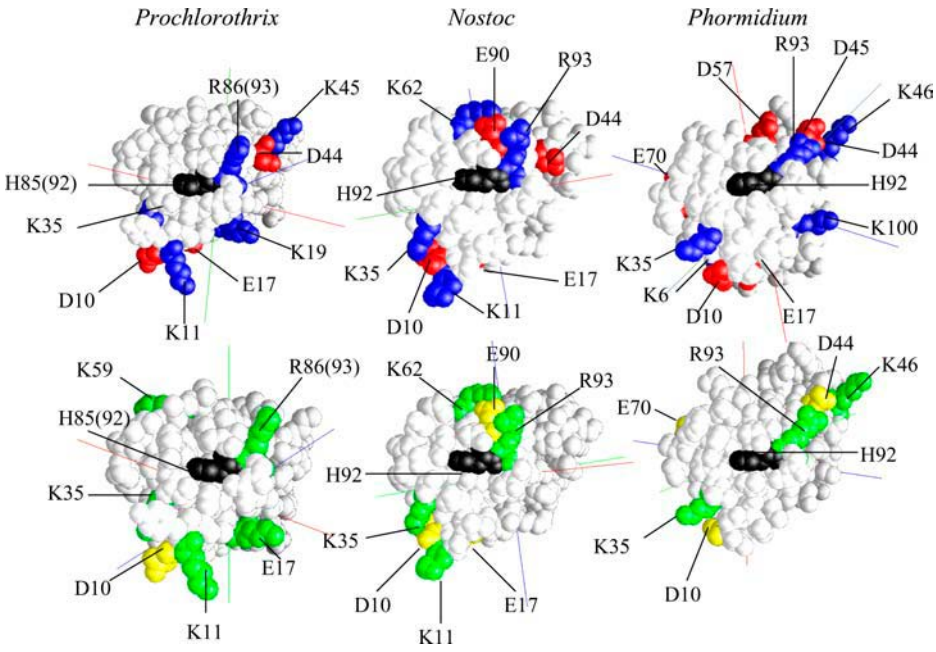

FIGURE 5 Location of charged amino acid residues involved in complex formation for *Prochlorothrix*, *Nostoc*, and *Phormidium* PC. (*Top*) Residues involved in complex formation as shown by mutational studies. *Prochlorothrix* PC: Residues found in Classes *I*, *II*, and *V* of Table 1 + K45. *Nostoc* PC: Residues found in Classes *I*, *II*, and *V* of Table 2. *Phormidium* PC: Residues found in Classes *I* and *V* from Table 2 from Gross (35). (*Black*, H92; *blue*, cationic residues; and *red*, anionic residues.) (*Bottom*) Residues on PC than make >0.5 electrostatic contacts with *Phormidium* cyt *f*. (Cationic residues, *green*; and anionic residues, *yellow*.)

and anionic) lie in a circle surrounding H92 (consensus sequence; see Appendix) (Fig. 5).

The most prevalent electrostatic contacts for residues on *Phormidium* cyt *f* are listed in Table 4. A residue is listed if it showed at least an average of 0.5 contacts/complex for at least one of the PC species represented. The following residues show at least 0.9 contacts/complex for all three PCs: D63, E123, R157, E165, D188, and the heme. All of these residues surround the heme as shown in Fig. 6. E165 and D188 are located on the small domain whereas all of the other residues are located on the large domain of cyt *f*.

Characteristics of complexes formed between *Phormidium* cyt *f* and PCs from different species of cyanobacteria

Heterogeneity of the complexes formed

The heterogeneity of the complexes formed is compared in Fig. 7 for complexes formed between *Phormidium* cyt *f* and PCs from *Nostoc*, *Phormidium*, and both WT and the Y12G mutant of *Prochlorothrix*. In each case, five complexes were chosen at random from those in which the Cu-Fe distance was less than the Cu-Fe distance at which the greatest number of complexes was observed. Considerable heterogeneity in the structure of the complexes was observed in all cases, except for the Y12G mutant of *Prochlorothrix* PC. There is less conformational heterogeneity than Crowley et al. (38) found for the double mutant Y12G-P14L, based on their NMR studies. Thus, these complexes are different from those previously observed between *Chlamydomonas* cyt *f* and *Chlamydomonas* PC (43), which showed considerable homogeneity in complex formation.

Structure of the cyanobacterial cyt f*-PC complexes*

Typical complexes are shown in Fig. 8 for *Phormidium* cyt *f* interacting with *Prochlorothrix* Y12G-PC. The mutant was chosen because the complexes were the most uniform of those studied and, thus, the structure represents that of a typical complex. The left-hand set of views is perpendicular to the long axis of cyt *f* and the right-hand view is looking down the long axis from the viewpoint of the small domain. As in the case of the *Phormidium* cyt *f*-*Phormidium* PC NMR complexes reported previously (37), the PC sits vertically on cyt *f* in contrast with both the BD simulations for *Chlamydomonas* PC interacting with *Chlamydomonas* cyt *f* (43) and the NMR results for spinach PC interacting with turnip cyt *f* (69) in which PC is slanted toward the small domain of cyt *f*. However, the view looking down the length of cyt *f* shows that the PC binding site is located toward the front side of cyt *f* where the heme and Y1 are located.

Residues K11, K35, and R93 interact with cyt *f* in agreement with the results of the mutant and electrostatic contact studies. D10 and E17 also lie close to the surface of cyt *f* where they cause electrostatic repulsion leading to a decrease in complex formation and the associated reaction rates. D63, E123, E165, and D188 on *Phormidium* cyt *f* interact with cationic residues on PC.

DISCUSSION

Evaluation of the MacroDox program

MacroDox is a very useful program for studying electrostatic interactions between proteins. In particular, it can predict the effects of mutations and determine the structure of the

TABLE 3 Electrostatic close contacts for cyanobacterial PCs interacting with *Phormidium* cyt *f*

PC	Residue	Number of contacts/complex formed*
Prochlorothrix†		
	D10	**1.43 ± 0.05**
	K11	**2.47 ± 0.08**
	K19	0.65 ± 0.01
	K35	**2.79 ± 0.05**
	K59 [63]	0.55 ± 0.05
	R88[93]	**4.21 ± 0.10**
Nostoc‡		
	K11	**2.10 ± 0.03**
	K35	**1.00 ± 0.05**
	K62	1.77 ± 0.05
	E90	2.09 ± 0.05
	R93	**3.30 ± 0.04**
Phormidium§		
	D10	**0.87 ± 0.07**
	K35	**2.55 ± 0.06**
	D44	0.81 ± 0.08
	K46	0.72 ± 0.07
	E70	0.93 ± 0.06
	R93	**2.18 ± 0.05**

*The number of electrostatic contacts was taken from the tabulation of the 15 closest electrostatic contacts listed for each complex in the MacroDox output .rec files that met a preset reaction criterion, which was a Cu-Fe distance less than or equal to the peak value for complex formation. To be listed, the average number of contacts per complex formed was ≥0.5. The conserved residues are in bold.

†*Prochlorothrix* PC: 193.0 ± 2.1 complexes were formed with a Cu-Fe distance ≤18 Å in five sets of 1000 trajectories each.

‡*Nostoc* PC: 139.8 ± 2.8 complexes were formed with a Cu-Fe distance of ≤17 Å in five sets of 1000 trajectories each.

§*Phormidium* PC: 104.0 ± 2.8 complexes were formed with a Cu-Fe distance of ≤20 Å in five sets of 5000 trajectories each.

complexes formed, which, in turn, provides the basis for further experiments. It requires relatively little computational time per simulation so that a large number of conditions (mutations, different ionic strengths, etc.) can be studied in a brief time. Steric effects can also be examined since both molecules have irregular geometrical shapes taken from the PDB files. For example, MacroDox was able to distinguish between wild-type and the Y12G mutant of *Prochlorothrix* PC interacting with *Phormidium* cyt *f* (Fig. 2 *B*). However, there are some serious limitations which are discussed in detail in Gross and Pearson (43) and Gross (35). The most serious considerations are:

1. The use of rigid structures in the simulations.
2. The use of a preset reaction criterion such as Cu-Fe distance.
3. The use of a high internal dielectric constant for Molecule II (PC) (36,59).
4. The neglect of desolvation effects (60).

Agreement of BD simulations and experimental results

The question arises as to how well the BD results agree with experiments both with respect to rates of electron transfer, and the structure of the complexes formed.

TABLE 4 Electrostatic close contacts for *Phormidium* cyt *f* interacting with cyanobacterial PCs

	Number of contacts/complex formed†		
Residue*	*Phormidium*‡	*Nostoc*	*Prochlorothrix*
D63	**2.51 ± 0.05**	**2.81 ± 0.03**	**2.34 ± 0.03**
E86	0.60 ± 0.09§	0.49 ± 0.05	0.18 ± 0.01
D108	0.94 ± 0.07	0.85 ± 0.06	0.48 ± 0.03
D122	0.35 ± 0.07	0.53 ± 0.03	0.92 ± 0.01
E123	**0.94 ± 0.06**	**1.16 ± 0.05**	**1.12 ± 0.02**
R157	**1.28 ± 0.03**	**1.38 ± 0.05**	**0.97 ± 0.03**
E165	**1.23 ± 0.05**	**0.92 ± 0.04**	**1.43 ± 0.03**
D188	**1.48 ± 0.05**	**1.75 ± 0.03**	**1.37 ± 0.05**
D205	0.06 ± 0.27	0.28 ± 0.10	0.87 ± 0.04
Heme	**3.49 ± 0.04**	**4.28 ± 0.03**	**4.00 ± 0.07**

Phormidium: 104.0 ± 2.8 complexes were formed with a Cu-Fe distance ≤20 Å (the peak of the plot of number of complexes formed versus Cu-Fe distance) in five sets of 5000 trajectories each. *Nostoc*: 139.8 ± 2.8 complexes were formed with a Cu-Fe distance of ≤17 Å in five sets of 1000 trajectories each. *Prochlorothrix*: 193.0 ± 2.1 complexes were formed with a Cu-Fe distance ≤18 Å in five sets of 1000 trajectories each.

*Consensus sequence.

†The number of electrostatic contacts were taken from the tabulation of the 15 closest electrostatic contacts found in the .rec files. Other conditions were as in Methods.

‡A residue was included in the table if the number of contacts/complex exceeded 0.5 for at least one species of PC tested. Those for which the number of contacts/complex exceeded 0.9 for all three species of PC are shown in bold.

With respect to the rates, three questions need to be answered:

1. Are the experimental rates diffusion- or activation-limited or have contributions of both?
2. Are the results of MacroDox simulations solely diffusion-limited?
3. How do the assumptions used in the MacroDox program affect the rates obtained?

With respect to the first question, Schlarb-Ridley et al. (55) studied the effect of viscosity and temperature on electron transfer rates for *Phormidium* cyt *f* interacting with *Phormidium* PC. They concluded that the reaction is not diffusion-limited, but instead involves a rearrangement of the initial diffusion-controlled complex to bring PC to a position

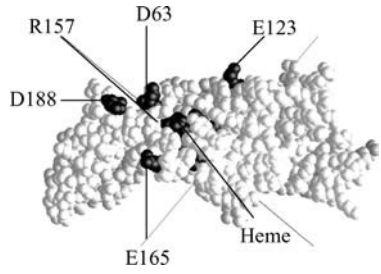

FIGURE 6 Location of residues on *Phormidium* cyt *f* that show >0.9 electrostatic contacts per complex formed for all three plastocyanins (*Prochlorothrix*, *Phormidium*, and *Anabaena* PC). The conditions are described for Table 4 and in Methods.

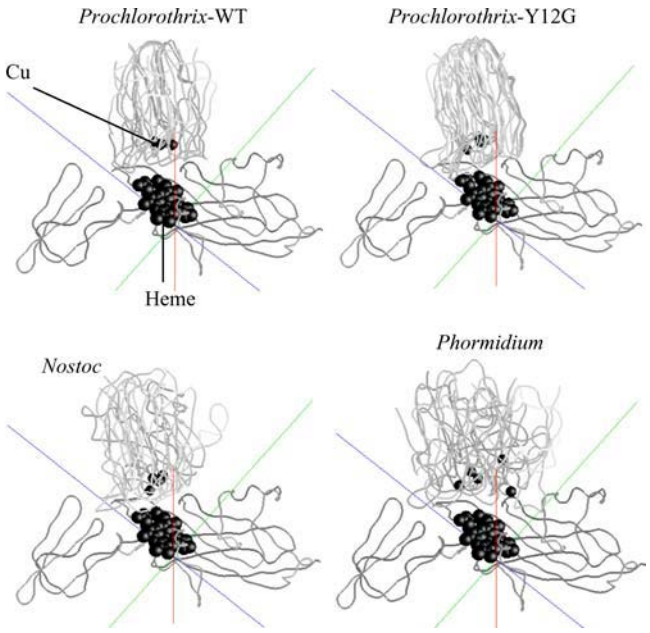

FIGURE 7 Homogeneity of complex formation for *Phormidium* cyt *f* interacting with various cyanobacterial PCs. Five complexes were selected at random from the 5000 (5 × 1000) trajectories per experiment for *Nostoc* and *Prochlorothrix* PC and from the 25,000 trajectories run for *Phormidium* PC. The only criterion used was that the Cu-Fe distance be less than the mean of the peaks shown in Fig. 2.

in which it can rapidly receive an electron from cyt *f*. Thus, the overall reaction is at least partially activation-limited.

The second question concerns whether the MacroDox complexes observed in our simulations are the result of diffusion or activation-limited processes. This depends on the reaction criterion used. If the reaction criterion used is best electrostatic interactions, then the complexes observed will be entirely electrostatically driven and diffusion-limited. On the other hand, the use of minimum Cu-Fe distance as the reaction criterion yields complexes as they would appear after a rearrangement with a small Cu-Fe distance allowing rapid electron transfer.

In the case of cyt *f* and PC, hydrophobic residues on both proteins would be brought together. Thus, although hydrophobic forces do not provide a driving force for complex formation, they are evident in the final complexes. However, the MacroDox complexes do not represent the final electron-transfer-active dock because many of them stop short of the final docked position (because of the random forces and the lack of an explicit inclusion of hydrophobic forces). This is the reason that hydrophobic interaction energies are underestimated.

With respect to question three, the magnitude of the rate constants determined by MacroDox simulations are always greater than the corresponding experimental values.

There are at least three reasons for the larger rate constants in MacroDox simulations. First, the rate constants for the simulations are overestimated due to the absence of a low internal dielectric constant for PC and the desolvation effects mentioned above. Second, no attempt was made to correct the BD reaction rates for attenuation due to the distance between the metal centers, which would decrease the measured electron transfer reaction rates (52,53). Third, the calculated rates are a function of the reaction coordinate cutoff distance. For these simulations, a 20 Å cutoff distance was chosen to include all possible complexes in which the Cu on PC might come close enough via electrostatic or hydrophobic interactions to receive an electron from cyt *f*. The 20 Å cutoff distance resulted in a calculated reaction rate (k_a) of 360×10^6 M^{-1} s^{-1} (35). Decreasing Cu-Fe reaction criterion distance to 18 Å (35) decreased the calculated rate to 80×10^6 M^{-1} s^{-1}, which is comparable to the experimental value of 47×10^6 M^{-1} s^{-1} (34).

The most important point, however, is that the relative effects of the mutations are independent of the reaction coordinate cutoff distance and are in general agreement with experiments, not only for mutations of *Phormidium* PC (34) but also for *Chlamydomonas* PC (44) when compared to experimental mutations of higher plant PCs (19,21). Thus, MacroDox simulations can be used to predict the effects of PC mutations in systems for which there are no experimental data.

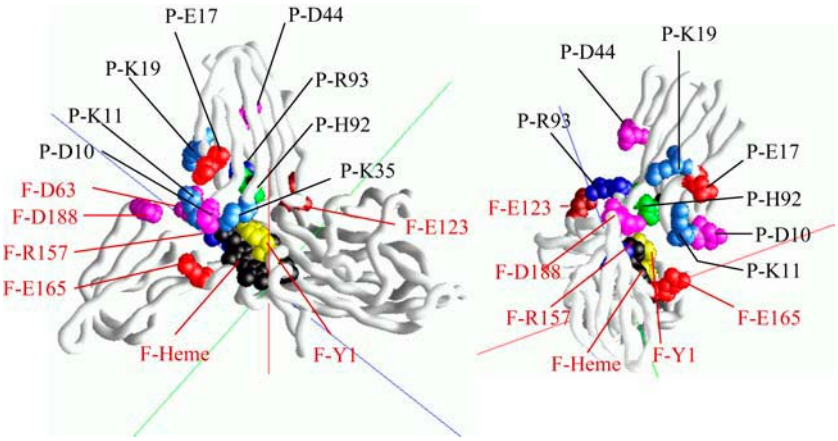

FIGURE 8 Typical BD complex between *Phormidium* cyt *f* and *Prochlorothrix* PC mutant Y12G. The complex shown is one of those chosen for Fig. 7. (PC residues are labeled in *black*; cyt *f* residues are labeled in *red*. Heme, *black*; cyt *f*-Y1, *yellow*; PC-H92, *green*; lysine, *light blue*; arginine, *dark blue*; aspartate, *magenta*; and glutamate, *red*.)

Overall, the structures of the BD complexes formed also agree with those determined by NMR. For example, the complex formed between *Chlamydomonas* PC and *Chlamydomonas* cyt *f* is very similar to that of spinach (69), poplar (71), and parsley (72) PC. In all of these cases, H87 (H92 in the cyanobacteria) faces the heme on cyt *f* and the PC molecule is tilted toward the small subunit with the two acidic clusters on PC interacting with the cationic residues on cyt *f*.

In contrast, in the complexes formed between *Phormidium* cyt *f* and *Phormidium* PC (35), *Prochlorothrix* PC (Figs. 7 and 8), and *Nostoc* PC (Fig. 7) PC, the PC molecules sits vertically on top of the cyt *f* with its long axis perpendicular to the long axis of cyt *f*. These results agree with the NMR results of Crowley et al. (37,38) for complexes formed between *Phormidium* cyt *f* and *Phormidium* and *Prochlorothrix* PC, respectively.

The role of electrostatic interactions in complexes formed between cytochrome *f* and PC in cyanobacteria

Electrostatic interactions between *Phormidium* cyt *f* and various cyanobacterial PCs depend on two factors: 1), the net charge on the PC molecule; and 2), the charge configuration around H92.

The effect of the net charge on the cyanobacterial PC molecule on complex formation

The results depicted in Fig. 3 show that the number of complexes formed in MacroDox simulations is a linear function of the net charge on the PC molecule whether the net charge on the PC molecule is altered by mutation or by using PCs from different species of cyanobacteria. Those species of cyanobacteria for which the net charge on PC at pH 7.0 is <-1.0, such as *Synechococcus*, *Synechocystis*, and *Phormidium*, show few if any complexes due to weaker electrostatic interactions in the Brownian dynamics (BD) simulations (note that there may still be complex formation due to hydrophobic interactions). These results agree with the NMR studies of complex formation between *Phormidium* cyt *f* and *Phormidium* PC (37), in which there was no effect of ionic strength on complex formation to indicate a paucity of electrostatic interactions. In contrast, cyanobacterial PCs having net charges more positive than -1.0, including WT *Nostoc* PC (net charge $= +1.1$) and *Prochlorothrix* PC (net charge $= +1.0$), showed a linear relationship between the number of complexes formed and the net charge on the PC molecule. This is true both for the *Prochlorothrix* mutants shown here and the *Phormidium* mutants described by Gross (68). Also, NMR studies of complex formation between *Phormidium* cyt *f* and *Prochlorothrix* PC (38) showed an ionic strength-dependence of complex formation indicating significant electrostatic interactions in agreement with the BD results described above. Note that a linear dependence of electron transfer rate on net charge was also observed for higher plants (19).

The increase in the number of BD complexes formed as a function of increasing positive charge on the PC molecule parallels the increase in binding constants for *Phormidium* cyt *f*-cyanobacterial PC complexes determined by NMR spectroscopy. For example, the binding constant for *Phormidium* PC complexes was 0.3 mM^{-1} PC (37), 6 ± 2 mM^{-1} for *Prochlorothrix* PC (38), and 12 ± 1 mM^{-1} for *Nostoc* PC (73) interacting with *Phormidium* cyt *f*. The increase in both the number of BD complexes formed and the magnitude of the binding constants reflect the increase in electrostatic interactions.

Specific charge interactions between *Phormidium* cyt *f* and cyanobacterial PCs

There are also specific charge interactions that are superimposed upon the net charge effects and influence the structure of the complexes formed between *Phormidium* cyt *f* and cyanobacterial PCs. Mutation of R93 and K35 to alanine inhibits complex formation for *Prochlorothrix* PC (Table 1), *Nostoc* PC (Table 2), *Phormidium* PC (Table 2 from Gross (35)), and *Synechocystis PC* (not shown). Mutant studies also show that K11 is important in *Prochlorothrix* and *Nostoc* PC as is K62 in *Nostoc* PC. K35, R93, and K11 (present only in *Prochlorothrix* and *Nostoc* PC) also showed more than one electrostatic contact per complex formed (3). On the other hand, mutation of D10 and E17 stimulated complex formation in all four cyanobacteria. Removal of D44 in *Prochlorothrix*, *Nostoc*, and *Phormidium* PC and E56 in *Synechocystis* PC also stimulated complex formation. Additional residues that are involved include E90 in *Nostoc* PC, E70 in *Synechocystis* PC, and D45, D55, and E70 in *Phormidium* PC.

R93, K35, D10, E17, and a residue in the vicinity of D44 are highly conserved in cyanobacterial PCs. Moreover, all of these residues surround H92 on the top face of cyanobacterial PC molecules (Fig. 5) implying that this is the face presented to cyt *f* in agreement with the NMR results for *Phormidium* (37) and *Prochlorothrix* (38) PCs interacting with *Phormidium* cyt *f*. These results contrast with those obtained for higher plant and green algal PCs in both NMR (62,64,65) and BD simulations (35,40,43,44), in which the anionic residues surrounding Y88 (Y83 in green plant numbering) provide the electrostatic interactions.

The role of hydrophobic interactions in complex formation between *Phormidium* cyt *f* and cyanobacterial PCs

The question arises as to the role of hydrophobic interactions in complex formation. This is particularly important for those PCs such as *Synechococcus*, *Synechocystis*, and *Phormidium* that show poor electrostatic interactions. All PCs including

those from higher plants and green algae have a highly conserved hydrophobic patch surrounding H92 (H87 in higher plants and green algae) (8), which includes the following amino acid residues: G8, G12 (Y in *Prochlorothrix*), L14 (P in *Prochlorothrix*), F16 (Y in *Prochlorothrix*), Residue 36 (hydrophobic in cyanobacteria and G in higher plants and algae), P38, L64 (Y in green algae and some higher plant PCs such as parsley), P91, G94, A95, and G96, plus some other residues in individual PCs. Thus, hydrophobic interactions appear to be ubiquitous.

One of the weaknesses of MacroDox is that it does not explicitly include hydrophobic interactions. What this means is that hydrophobic interactions are not included as a driving force for complex formation (i.e., the number of complexes formed and the corresponding reaction rates would be greater upon inclusion of hydrophobic forces. This is particularly important in the case of mutants R93A (*Nostoc* PC) and R86A (*Prochlorothrix* PC) as well as wild-type *Phormidium*, *Synechocystis*, and *Synechococcus* PC, which would have shown significant complex formation if hydrophobic interactions had been included.

However, even though it was not possible to include hydrophobic interactions as a driving force for complex formation, it was possible to estimate the hydrophobic interaction energies of the complexes formed. The strength of the hydrophobic interactions was estimated for *Prochlorothrix*, *Nostoc*, and *Phormidium* PC interacting with *Phormidium* cyt *f* (Table 5). The procedure involved determining the surface areas of those residues involved in hydrophobic interactions between PC and cyt *f*. The surface areas of individual residues and atoms thereof for both cyt *f* and PC were determined using the method of Richards (62,63). Of these, the residues involved in hydrophobic interactions and the sum of their surface areas were determined as described in Methods and in Gross and Pearson (42). Two times the smaller of the two hydrophobic surface areas (PC or cyt *f*) was taken as the hydrophobic surface area given in Table 5.

There are two large sources of error in these calculations. The first involves measurement of the hydrophobic surface area involved in complex formation. If the MacroDox complexes has been the final-electron-transfer-active docks, then it would be a relatively simple matter to measure the contact area on both molecules. As it is, it is necessary to estimate the contact area which was easier to do for the relatively tight complexes of *Nostoc* and *Prochlorothrix* PC than for the looser complexes of *Phormidium* PC. As it was, the contact area was estimated as follows. Those residues on one protein (e.g., PC) were considered to be involved in final complex formation if they lay within 8 Å of a residue on the other protein (e.g., cyt *f*) in at least eight out of 10 of the complexes examined (seven out of 10 for *Phormidium* PC). This method underestimates the hydrophobic surface area, particularly in the case of *Phormidium* PC.

The second problem is that there are large uncertainties in the magnitude of the hydrophobic free energies with estimates varying from -25 to -47 cal/Å^2 (64–66), which is why we have used both values in our calculations (Table 5). Nonetheless, two conclusions can be drawn. First, the hydrophobic free energies are as large as, or larger than, the electrostatic free energies. For *Prochlorothrix* PC (Table 5), for example, the hydrophobic interaction energies using -25 cal/Å (64) was -16.1 kcal-mol^{-1} compared to -9.1 kcal-mol^{-1} for the electrostatic interaction energies. Second, the hydrophobic interaction energies are larger for the cyanobacteria than for *Chlamydomonas* (-7.5 kcal-mol^{-1}) (47). The results agree with the experimental results of Schlarb-Ridley et al. (74), who observed significant interactions between *Phormidium* PC and *Phormidium* cyt *f* even at infinite ionic strength. On the other hand, the magnitude of the electrostatic interactions was the same magnitude for *Nostoc* (-8.5 ± 0.3 kcal-mol^{-1}) and *Prochlorothrix* PC (-10.5 ± 0.4 kcal-mol^{-1}) as for *Chlamydomonas* PC (-10.5 ± 1.5 kcal-mol^{-1}), although the charge configurations are different. Note that the electrostatic interaction energy for *Phormidium* PC (-2.1 ± 0.4 kcal-mol^{-1}) was less, as expected, due to the lower net charge.

The structure of the complexes formed between *Phormidium* cyt *f* and cyanobacterial PCs

An examination of the residues involved in electrostatic contacts (Table 4, Fig. 6) shows that the binding site on cyt *f* for cyanobacterial PCs surrounds the heme with five of the most frequent electrostatic contacts (D63, E123, K157, and

TABLE 5 Hydrophobic and electrostatic free energies of the complexes formed

	PC	*Nostoc*	*WT Prochlorothrix*	*Y12G Prochlorothrix*	*Phormidium*	*Chlamydomonas**
	Cyt *f*	*Phormidium*	*Phormidium*	*Phormidium*	*Phormidium*	*Chlamydomonas*
		Hydrophobic interaction energies (kcal-mol^{-1})†				
	Hydrophobic surface area (Å^2)	690	646	826	313	300
Energy	Using -25 cal/Å^2	-17.2	-16.1	-20.6	-7.8	-7.5
	Using -47 cal/Å^2	-32.4	-30.3	-38.8	-14.7	-14.1
		Electrostatic interaction energies (kcal-mol^{-1})				
		-8.5 ± 0.3	-9.8 ± 0.5	-10.8 ± 0.4	-2.1 ± 0.4	-10.5 ± 1.5

*Taken from Gross and Pearson (43).
†Molecular surface areas, hydrophobic interaction energies, and electrostatic interaction energies were calculated as described in Methods.

E165, in addition to the heme itself) residing on the large domain and only D188 being situated on the small domain. In addition, the long axis of PC is perpendicular to the long axis of cyt *f* as shown previously for *Phormidium* cyt *f*-*Phormidium* PC and *Phormidium* cyt *f* -*Prochlorothrix* PC complexes in NMR studies (37,38) and by Gross (35) in BD simulations of *Phormidium* cyt *f* interacting with *Phormidium* PC. Thus, the structure of these complexes is different from those of higher plants and algae in which both NMR studies (69–72,75) and BD simulations (39,42,43) in which PC leans toward the small domain, allowing the lower negative patch to interact with positively-charged residues on the small domain of cyt *f* (e.g., K187 and K188 in *Chlamydomonas* cyt *f*).

However, all three PCs examined (WT *Prochlorothrix*, *Nostoc*, and *Phormidium*) showed considerable heterogeneity in orientation around the long axis of PC. The results for *Phormidium* PC agree with the NMR results of Crowley et al. (37), who also observed considerable heterogeneity of the complexes formed (See (35) for a comparison of BD and NMR results). These results are different from those for both higher plants and green algae where both NMR results (69) and BD simulations (43) showed more complexes that are homogeneous. This may be attributed to the greater asymmetry in charge distribution on PC molecules from higher plants and green algae (i.e., most of the negatively-charged residues are located on one face of the PC molecule). If charge asymmetry is required for orientation of PC within the complexes, then the more uniform electrostatic field around cyanobacterial PCs would not be expected to promote a single orientation of PC within the complexes. Interestingly, mutating Y12 to G increased the homogeneity of the complexes formed (Fig. 7). If the only requirement for electron transfer is a close distance between Y1 on cyt *f* and H92 (H87 in higher plants and green algae) on PC, then the orientation of PC within the complex is not important and multiple orientations of the PC molecule (provided H92 is close to Y1) may actually increase the probability of electron transfer as suggested by Crowley and Ubbink (70).

CONCLUSIONS

Unlike higher plant and green algal PCs, there is considerable variation in the electrostatic interactions between *Phormidium* cyt *f* and various cyanobacterial PCs. The ability to form electrostatic complexes is dependent both the net charge on the PC molecule and the distribution of charged residues surrounding H92 on the surface of the PC molecule. These involve interactions between positively-charged residues on PC such as K35 and R93 and negatively-charged residues on *Phormidium* cyt *f*, including D63, E123, E165, D188, and the heme. In addition to the electrostatic interactions, significant hydrophobic interactions are involved in complex formation.

The complexes formed for all three cyanobacterial PCs studied show heterogeneity in the orientation of the PC molecule on cyt *f* even in complexes where the H92 ligand to the Cu on PC is close to the Y1 ligand to the heme on cyt *f*. These results suggest that an exact orientation is not required for electron transfer.

APPENDIX

The numbering used throughout is the numbering from the PDB file of *Nostoc* PC. In this system, H92 on the cyanobacterial PCs corresponds to H87 in higher plant and algal PCs. The numbering for the other cyanobacterial PCs is found in brackets in the tables and in the text. The sequences were aligned using Deep View from Swiss Prot (76), http://www.expasy.ch/spdbv/.

REFERENCES

1. Kurisu, G., H. Zhang, J. L. Smith, and W. A. Cramer. 2003. Structure of the cytochrome b_6f complex of oxygenic photosynthesis: tuning the cavity. *Science*. 302:1009–1014.
2. Stroebel, D., Y. Choquet, J. L. Popot, and D. Picot. 2003. An atypical haem in the cytochrome b_6f complex. *Nature*. 426:399–400.
3. Smith, J. L., H. Zhang, J. Yan, G. Kurisu, and W. A. Cramer. 2004. Cytochrome *bc* complexes: a common core of structure and function surrounded by diversity in the outlying provinces. *Curr. Opin. Struct. Biol.* 14:432–439.
4. Cramer, W. A., H. Zhang, J. Yan, G. Kurisu, and J. L. Smith. 2004. Evolution of photosynthesis: time-independent structure of the cytochrome b_6f complex. *Biochemistry*. 43:5921–5929.
5. Freeman, H. C. 1981. Electron transfer in ''blue'' copper proteins. *Chord Chem.* 21:29–52.
6. Sykes, A. G. 1991. Plastocyanin and the blue copper proteins. *Struct. Bond.* 75:175–224.
7. Gross, E. L. 1993. Plastocyanin: structure and function. *Photosynth. Res.* 37:103–116.
8. Gross, E. L. 1996. Plastocyanin: structure, location, diffusion, and electron transfer mechanisms. *In* Oxygenic Photosynthesis: The Light Reactions. D. Ort and C. Yocum, editors. Kluwer Academic Publishers, Dordrecht, the Netherlands. 413–429.
9. Redinbo, M. R., T. O. Yeates, and S. Merchant. 1994. Plastocyanin: structural and functional analysis. *J. Bioenerg. Biomembr.* 26:49–66.
10. Sigfridsson, K. 1998. Plastocyanin, an electron-transfer protein. *Photosynth. Res.* 57:1–28.
11. Hope, A. B. 2000. Electron transfers amongst cytochrome *f*, plastocyanin and Photosystem I: kinetics and mechanisms. *Biochim. Biophys. Acta.* 1456:5–26.
12. Takenaka, K., and T. Takabe. 1984. Importance of local positive charges on cytochrome *f* for electron transfer to plastocyanin and potassium ferricyanide. *J. Biochem.* (*Tokyo*). 96:1813–1821.
13. Takabe, T., K. Takenaka, H. Kawamura, and Y. Beppu. 1986. Charges on proteins and distances of electron transfer in metalloprotein redox reactions. *J. Biochem.* (*Tokyo*). 99:833–840.
14. Anderson, G. P., D. G. Sanderson, C. H. Lee, S. Durell, L. B. Anderson, and E. L. Gross. 1987. The effect of ethylene diamine chemical modification of plastocyanin on the rate of cytochrome *f* oxidation and P-700$^+$ reduction. *Biochim. Biophys. Acta.* 894:386–398.
15. Morand, L. Z., M. K. Frame, K. K. Colvert, D. A. Johnson, D. W. Krogmann, and D. J. Davis. 1989. Plastocyanin cytochrome *f* interaction. *Biochemistry*. 28:8039–8047.
16. Takabe, T., and H. Ishikawa. 1989. Kinetic studies on a cross-linked complex between plastocyanin and cytochrome *f*. *J. Biochem.* (*Tokyo*). 105:98–102.

17. Qin, L., and N. M. Kostic. 1993. Importance of protein rearrangement in the electron-transfer reaction between the physiological partners cytochrome *f* and plastocyanin. *Biochemistry*. 32:6073–6080.

18. Lee, B. H., T. Hibino, T. Takabe, P. J. Weisbeek, and T. Takabe. 1995. Site-directed mutagenesis study on the role of negative patches on silane plastocyanin in the interactions with cytochrome *f* and photosystem I. *J. Biochem.* (*Tokyo*). 117:1209–1217.

19. Kannt, A., S. Young, and D. S. Bendall. 1996. The role of acidic residues of plastocyanin in its interaction with cytochrome *f*. *Biochim. Biophys. Acta*. 1277:115–126.

20. Soriano, G. M., M. V. Pomamarev, R. A. Piskorowski, and W. A. Cramer. 1998. Identification of the basic residues of cytochrome *f* responsible for electrostatic docking interactions with plastocyanin *in vitro*: relevance to the electron transfer reaction *in vivo*. *Biochemistry*. 37:15120–15128.

21. Gong, E. S., J. Q. Wen, N. E. Fisher, S. Young, C. J. Howe, D. S. Bendall, and J. C. Gray. 2000. The role of individual lysine residues in the basic patch on turnip cytochrome *f* for the electrostatic interactions with plastocyanin *in vitro*. *Eur. J. Biochem.* 267:3461–3468.

22. Soriano, G. M., M. V. Ponamarev, G. S. Tae, and W. A. Cramer. 1996. Effects of the interdomain basic region of cytochrome *f* on its redox reactions in vivo. *Biochemistry*. 35:14590–14598.

23. Pearson, D. C., Jr., E. L. Gross, and E. S. David. 1996. The electrostatic properties of cytochrome *f*: Implications for docking with plastocyanin. *Biophys. J*. 71:64–76.

24. Gray, J. C. 1992. Cytochrome *f*: structure, function and biosynthesis. *Photosynth. Res.* 34:359–374.

25. Martinez, S. E., D. Huang, A. Szczepaniak, W. A. Cramer, and J. L. Smith. 1994. Crystal structure of the chloroplast cytochrome *f* reveals a novel cytochrome fold and unexpected heme ligation. *Structure*. 2:95–105.

26. Martinez, S. E., D. Huang, M. Ponomarev, W. A. Cramer, and J. L. Smith. 1996. The heme redox center of chloroplast cytochrome *f* is linked to a buried five-water chain. *Protein Sci.* 5:1081–1092.

27. Durell, S. R., J. K. Labanowski, and E. L. Gross. 1990. Modeling of the electrostatic potential field of plastocyanin. *Arch. Biochem. Biophys.* 277:241–254.

28. Carrell, C. J., B. G. Schlarb, D. S. Bendall, C. J. Howe, W. A. Cramer, and J. L. Smith. 1999. Structure of the soluble domain of cytochrome *f* from the cyanobacterium *Phormidium laminosum*. *Biochemistry*. 38: 9590–9599.

29. Badsburg, U., A. M. Jorgensen, H. Gesmar, J. J. Led, J. M. Hammerstad, L. L. Jespersen, and J. Ulstrop. 1996. Solution structure of reduced plastocyanin from the blue-green alga *Anabaena variables*. *Biochemistry*. 35:7021–7031.

30. Babu, C. R., B. F. Volkman, and G. S. Bullerjahn. 1999. NMR solution structure of plastocyanin from the photosynthetic prokaryote, *Prochlorothrix hollandica*. *Biochemistry*. 38:4988–4995.

31. Bond, C. S., D. S. Bendall, H. C. Freeman, J. M. Guss, C. J. Howe, M. J. Wagner, and M. C. Wilce. 1999. The structure of plastocyanin from the cyanobacterium *Phormidium laminosum*. *Acta Crystallogr.* D55:414–421.

32. Bertini, I., S. Ciurli, A. Dikiy, C. O. Fernandez, C. Luchinat, N. Safarov, S. Shumilin, and A. J. Vila. 2001. The first solution structure of a paramagnetic copper(II) protein: the case of oxidized plastocyanin from the cyanobacterium *Synechocystis* PCC6803. *J. Am. Chem. Soc.* 123:2405–2413.

33. Inoue, T., H. Sugawara, S. Hamanaka, H. Tsukui, E. Suzuki, T. Kohzuma, and Y. Kai. 1999. Crystal structure determinations of oxidized and reduced plastocyanin from the cyanobacterial *Synechococcus* sp. PCC 7942. *Biochemistry*. 38:6063–6069.

34. Schlarb-Ridley, B. G., D. S. Bendall, and C. J. Howe. 2002. Role of electrostatics in the interaction between cytochrome *f* and plastocyanin of the cyanobacterium *Phormidium laminosum*. *Biochemistry*. 279: 3279–3285.

35. Gross, E. L. 2004. A Brownian dynamics study of the interaction of *Phormidium laminosum* plastocyanin with *Phormidium laminosum* cytochrome *f*. *Biophys. J*. 87:2043–2059.

36. Northrup, S. H., K. A. Thomasson, C. M. Miller, P. D. Barker, L. D. Eltis, J. G. Guillemette, S. C. Inglis, and A. G. Mauk. 1993. Effect of charged amino acid mutations on the bimolecular kinetics of reduction of yeast iso-1-ferricytochrome *c* by bovine ferricytochrome b_5. *Biochemistry*. 32:6613–6623.

37. Crowley, P. B., G. Otting, B. G. Schlarb-Ridley, G. W. Canters, and M. Ubbink. 2001. Hydrophobic interactions in a cyanobacterial plastocyanin-cytochrome *f* complex. *J. Am. Chem. Soc.* 123:10444–10453.

38. Crowley, P. B., N. Vintonenko, G. S. Bullerjahn, and M. Ubbink. 2002. Plastocyanin-cytochrome *f* interactions: the influence of hydrophobic patch mutations studied by NMR spectroscopy. *Biochemistry*. 41:15698–15705.

39. Gabdoulline, R. R., and R. C. Wade. 2002. Biomolecular diffusional association. *Curr. Opin. Struct. Biol*. 12:204–213.

40. Pearson, D. C., Jr., and E. L. Gross. 1998. Brownian dynamics study of the interaction between plastocyanin and cytochrome *f*. *Biophys. J*. 75:2698–2711.

41. Nelson, N., D. C. Pearson, Jr., and E. L. Gross. 1999. The interaction of plastocyanin with cytochrome *f*: a Brownian dynamics study. *In* Photosynthesis: Mechanisms and Effects, Vol. III. G. Garab, editor. Kluwer Academic Publishers, Dordrecht, The Netherlands. 1493–1498.

42. De Rienzo, F., R. R. Gabdoulline, M. C. Menziani, P. G. De Benedetti, and R. C. Wade. 2001. Electrostatic analysis and Brownian dynamics simulation of the association of plastocyanin and cytochrome *f*. *Biophys. J*. 81:3090–3104.

43. Gross, E. L., and D. C. Pearson, Jr. 2003. Brownian Dynamics simulations of the interaction of *Chlamydomonas* cytochrome *f* with plastocyanin and cytochrome c_6. *Biophys. J*. 85:2055–2068.

44. Haddadian, E. J., and E. L. Gross. 2005. Brownian dynamics study of cytochrome *f* interactions with cytochrome c_6 and plastocyanin in *Chlamydomonas reinhardtii*, plastocyanin and cytochrome c_6 mutants. *Biophys. J*. 88:2323–2339.

45. Berman, H. M., J. Westboro, Z. Feng, G. Gilliland, T. N. Bhat, H. Weissig, I. N. Shindyalov, and P. E. Bourne. 2000. The Protein Data Bank. *Nucleic Acids Res.* 28:235–242.

46. Chi, Y. I., L. S. Huang, Z. Zhang, J. G. Fernandez-Velasco, and E. A. Berry. 2000. X-ray structure of a truncated form of cytochrome f from *Chlamydomonas reinhardtii*. *Biochemistry*. 39:7689–7701.

47. Redinbo, M. R., D. Cascio, M. K. Choukair, D. Rice, S. Merchant, and T. O. Yeates. 1993. The 1.5-Å crystal structure of plastocyanin from the green alga *Chlamydomonas reinhardtii*. *Biochemistry*. 32:10560–10567.

48. Northrup, S. H., J. O. Boles, and J. C. L. Reynolds. 1987. Electrostatic effects in the Brownian dynamics of association and orientation of heme proteins. *J. Phys. Chem.* 91:5991–5998.

49. Northrup, S. H. 1999. MacroDox v.2.3.1: Software for the Prediction of Macromolecular Interaction. Tennessee Technological University, Cookeville, TN.

50. Nicholls, A., and B. Honig. 1991. A rapid finite-difference algorithm, utilizing successive over relaxation to solve the Poisson-Boltzmann equation. *J. Comput. Chem.* 12:435–445.

51. Pearson, D. C., Jr. 2000. Brownian dynamics study of the interaction between cytochrome *f* and mobile electron transfer proteins. PhD dissertation. The Ohio State University, Columbus, OH.

52. Moser, C. C., J. M. Keske, K. Warncke, R. S. Farid, and P. L. Dutton. 1992. Nature of biological electron transfer. *Nature*. 355:796–802.

53. Moser, C. C., C. C. Page, R. Farid, and P. L. Dutton. 1995. Biological electron transfer. *J. Bioenerg. Biomembr.* 27:263–274.

54. Hart, S. E., B. G. Schlarb-Ridley, C. Delon, D. S. Bendall, and C. J. Howe. 2003. Role of the charges on cytochrome *f* from the cyanobacterium *Phormidium laminosum* in its interactions Plastocyanin. *Biochemistry*. 42:4829–4836.

55. Schlarb-Ridley, B. G., H. Mi, W. D. Teale, V. S. Meyer, C. J. Howe, and D. S. Bendall. 2005. Implications of the effects of viscosity, macromolecular crowding and temperature for the transient interaction between cytochrome *f* and plastocyanin from the cyanobacterium *Phormidium laminosum*. *Biochemistry*. 44:6232–6238.

56. Matthew, J. B. 1985. Electrostatic effects in proteins. *Annu. Rev. Biophys. Biophys. Chem.* 14:387–417.

57. Warwicker, J., and H. C. Watson. 1982. Calculation of the electric potential in the active site cleft due to α-helix dipoles. *J. Mol. Biol.* 157:671–679.

58. Gabdoulline, R. R., and J. C. Wade. 1998. Brownian dynamics simulation of protein-protein diffusional encounter. *Methods.* 14:329–341.

59. Gabdoulline, R. R., and J. C. Wade. 2001. Protein-protein association: investigation of factors influencing association rates by Brownian dynamics simulations. *J. Mol. Biol.* 9:1139–1155.

60. Elcock, A. H., R. R. Gabdoulline, R. C. Wade, and J. A. McCammon. 1999. Computer simulation of protein-protein kinetics: acetylcholinesterase-fasciculin. *J. Mol. Biol.* 291:149–162.

61. Northrup, S. H. 1996. Theoretical simulation of protein-protein interactions. *In* Cytochrome *c*: A Multidisciplinary Approach. R.A. Scott and A.G. Mauk, editors. University Science Publishers, Sausalito, CA. 543–570.

62. Lee, B., and F. M. Richards. 1971. The interpretation of protein structures: estimation of static accessibility. *J. Mol. Biol.* 55:379–400.

63. Richards, F. M. 1977. Areas, volumes, packing, and protein structure. *Annu. Rev. Biophys. Bioeng.* 6:151–176.

64. Janin, J., and C. Chothia. 1990. The structure of protein-protein recognition sites. *J. Biol. Chem.* 265:16027–16030.

65. Rose, G. D., and R. Wolfenden. 1993. Hydrogen bonding, hydrophobicity, packing and protein folding. *Annu. Rev. Biophys. Biomol. Struct.* 22:381–415.

66. Sharp, K. A., A. Nicholls, R. F. Fine, and B. Honig. 1991. Reconciling the magnitude of the microscopic and macroscopic hydrophobic effects. *Science.* 252:106–109.

67. Schwede, T., J. Kopp, N. Guex, and M. C. Peitsch. 2003. SWISS-MODEL: an automated protein homology-modeling server. *Nucleic Acids Res.* 31:3381–3385.

68. Gross, E. L. 2005. Brownian dynamics studies of the interaction of cyanobacterial plastocyanins with cytochrome *f*. *In* Proceedings of the 13th International Congress on Photosynthesis, Montreal, Canada, August 29-September 3, 2004. In press.

69. Ubbink, M., M. Ejdebäck, B. G. Karlsson, and D. S. Bendall. 1998. The structure of the complex of plastocyanin and cytochrome *f*, determined by paramagnetic NMR and restrained rigid-body molecular dynamics. *Structure.* 6:323–335.

70. Crowley, P. B., and M. Ubbink. 2003. Close encounters of the transient kind: protein interactions in the photosynthetic redox chain investigated by NMR spectroscopy. *Acc. Chem. Res.* 36:723–730.

71. Lange, C., T. Cornvik, I. Diaz-Moreno, and M. Ubbink. 2005. The transient complex of poplar plastocyanin with cytochrome *f*: effects of ionic strength and pH. *Biochim. Biophys. Acta.* 1707:179–188.

72. Crowley, P. B., D. M. Hunter, K. Sato, W. McFarlane, and C. Dennison. 2004. The parsley plastocyanin-turnip cytochrome *f* complex: a structurally distorted but kinetically functional acidic patch. *Biochem. J.* 378:45–51.

73. Diaz-Moreno, I., A. Diaz-Quintana, M. A. De la Rosa, P. B. Crowley, and M. Ubbink. 2005. Different modes of interaction in cyanobacterial complexes of plastocyanin and cytochrome *f*. *Biochemistry.* 44:3176–3183.

74. Schlarb-Ridley, B. G., D. S. Bendall, and C. J. Howe. 2003. Relation between interface properties and kinetics of electron transfer in the interaction of cytochrome *f* and plastocyanin from plants and the cyanobacterium *Phormidium laminosum*. *Biochemistry.* 42:4057–4063.

75. Ejdebäck, M., A. Bergkvist, B. G. Karlsson, and M. Ubbink. 2000. Side-chain interactions in the plastocyanin-cytochrome *f* complex. *Biochemistry.* 39:5022–5027.

76. Guex, N., and M. C. Peitsch. 1997. SWISS-MODEL and the Swiss-PDB Viewer: an environment for comparative protein modeling. *Electrophoresis.* 18:2714–2723.